



LJMU Research Online

McGee, SL, Balogh, ML, Bower, RG, Font, AS and McCarthy, IG

The accretion of galaxies into groups and clusters

<http://researchonline.ljmu.ac.uk/id/eprint/1316/>

Article

Citation (please note it is advisable to refer to the publisher's version if you intend to cite from this work)

McGee, SL, Balogh, ML, Bower, RG, Font, AS and McCarthy, IG (2009) The accretion of galaxies into groups and clusters. MONTHLY NOTICES OF THE ROYAL ASTRONOMICAL SOCIETY, 400 (2). pp. 937-950. ISSN 0035-8711

LJMU has developed **LJMU Research Online** for users to access the research output of the University more effectively. Copyright © and Moral Rights for the papers on this site are retained by the individual authors and/or other copyright owners. Users may download and/or print one copy of any article(s) in LJMU Research Online to facilitate their private study or for non-commercial research. You may not engage in further distribution of the material or use it for any profit-making activities or any commercial gain.

The version presented here may differ from the published version or from the version of the record. Please see the repository URL above for details on accessing the published version and note that access may require a subscription.

For more information please contact researchonline@ljmu.ac.uk

<http://researchonline.ljmu.ac.uk/>

The accretion of galaxies into groups and clusters

Sean L. McGee^{1*}, Michael L. Balogh¹, Richard G. Bower², Andreea S. Font²,
Ian G. McCarthy^{3,4,5}

¹*Department of Physics and Astronomy, University of Waterloo, Waterloo, Ontario, N2L 3G1, Canada*

²*Department of Physics, University of Durham, Durham, UK, DH1 3LE*

³*Kavli Institute for Cosmology, University of Cambridge, Cambridge, UK, CB3 0HA*

⁴*Astrophysics Group, Cavendish Laboratory, University of Cambridge, Cambridge, UK, CB3 0HE*

⁵*Institute of Astronomy, University of Cambridge, Cambridge, UK, CB3 0HA*

19 February 2013

ABSTRACT

We use the galaxy stellar mass and halo merger tree information from the semi-analytic model galaxy catalogue of Font et al. (2008) to examine the accretion of galaxies into a large sample of groups and clusters, covering a wide range in halo mass ($10^{12.9}$ to $10^{15.3} h^{-1} M_{\odot}$), and selected from each of four redshift epochs ($z=0, 0.5, 1.0$ and 1.5). We find that clusters at all examined redshifts have accreted a significant fraction of their final galaxy populations through galaxy groups. A $10^{14.5} h^{-1} M_{\odot}$ mass cluster at $z=0$ has, on average, accreted $\sim 40\%$ of its galaxies ($M_{\text{stellar}} > 10^9 h^{-1} M_{\odot}$) from halos with masses greater than $10^{13} h^{-1} M_{\odot}$. Further, the galaxies which are accreted through groups are more massive, on average, than galaxies accreted through smaller halos or from the field population. We find that at a given epoch, the fraction of galaxies accreted from isolated environments is independent of the final cluster or group mass. In contrast, we find that observing a cluster of the same halo mass at each redshift epoch implies different accretion rates of isolated galaxies, from 5–6 % per Gyr at $z=0$ to 15% per Gyr at $z=1.5$. We find that combining the existence of a Butcher Oemler effect at $z=0.5$ and the observations that galaxies within groups display significant environmental effects with galaxy accretion histories justifies striking conclusions. Namely, that the dominant environmental process must begin to occur in halos of $10^{12} - 10^{13} h^{-1} M_{\odot}$, and act over timescales of > 2 Gyrs. This argues in favor of a mechanism like “strangulation”, in which the hot halo of a galaxy is stripped upon infalling into a more massive halo. This simple model predicts that by $z=1.5$ galaxy groups and clusters will display little to no environmental effects. This conclusion may limit the effectiveness of red sequence cluster finding methods at high redshift.

Key words: galaxies: clusters: general, galaxies: evolution, galaxies: formation

1 INTRODUCTION

In recent years, an extraordinary confluence of independent measurements of the cosmological parameters has resulted in the concordance model of the Universe (Λ CDM), in which the mass density is dominated by cold dark matter. In this model, the initial distribution of density perturbations has the greatest power on small scales, which causes low mass dark matter haloes to form first at high redshift. Larger haloes form later through the merging, or accretion, of smaller halos. Eventually, this ‘hierarchical structure formation’ leads to the formation of galaxy groups and clusters, which become more common with time. The mass assembly of dark matter halos has been extensively stud-

ied analytically (Press & Schechter 1974; Bond et al. 1991; Bower 1991; Lacey & Cole 1993; Sheth & Tormen 2002; van den Bosch 2002; Benson et al. 2005) and through numerical simulations (Davis et al. 1985; Li et al. 2008). Consistent with these studies, Berrier et al. (2009, hereafter B09) used n-body simulations to show that the mass assembly of clusters is dominated by the most massive accretion events; in effect, the merging of groups with clusters. However, by associating dark matter subhalos with galaxies, they show that the *galaxy* assembly of clusters is dominated by lower mass halos, or the infalling of isolated galaxies. This distinction could be of great importance since there are a variety of physical processes that depend on the mass of the host dark matter halo and which could affect the properties of a galaxy, such as ram pressure stripping, strangulation and galaxy harassment.

Indeed, detailed observations of dense environments, galaxy groups, and clusters in the local universe have shown that the galax-

* Email: s2mcgee@uwaterloo.ca

ies which inhabit these environments have properties substantially different from galaxies in low density or field environments. In particular, galaxy groups and clusters have lower average galaxy star formation rates (Lewis et al. 2002; Gómez et al. 2003), lower fractions of disk galaxies (Dressler et al. 1997; McGee et al. 2008), and higher red fractions (Balogh et al. 2004; Weinmann et al. 2006) than field galaxies. Despite this wealth of observational data, there is no consensus on the dominant physical mechanism responsible for these differences, mainly because large populations of “transition” objects have avoided detection. In particular, there is no large excess in the fraction of galaxies between the red sequence and the blue cloud in dense environments (Balogh et al. 2004; Weinmann et al. 2006). While there are specific examples of transitioning spiral galaxies which are in the process of having their HI gas stripped due to ram pressure in local clusters (Kenney et al. 2004; Vollmer et al. 2004), the X-ray temperatures and pressures, as well as the infalling velocity of the galaxies, required for such a transformation mechanism are probably too high to be effective in low mass groups.

Strangulation, the process in which the more loosely bound hot halo of a galaxy is stripped by the group or cluster halo, leaving a reduced amount of gas available for future star formation (Balogh et al. 2000), is an attractive candidate because it is still effective in low mass groups (McCarthy et al. 2008b; Kawata & Mulchaey 2008). However, it is not clear if such a gentle mechanism can account for the dramatic effect seen in clusters. Zabludoff & Mulchaey (1998) have proposed that the extreme properties of galaxy clusters may result from the “pre-processing” of galaxies in group environments before accretion into the cluster. This is supported by observations of reduced star formation rates in the outskirts of clusters, well past the virial radius (Balogh et al. 1999; Lewis et al. 2002). However, B09 have claimed that “pre-processing” is not a large effect. They find only $\sim 12\%$ of galaxies are accreted in to the final cluster environment as members of groups with five or more galaxies. While the B09 clusters are relatively low mass, their work shows the importance of distinguishing the accretion of galaxies from that of dark matter mass.

A complementary approach to trying to isolate “transition galaxies” is to study the properties of galaxies in groups and clusters as a function of redshift. As first shown by Butcher & Oemler (1978) and confirmed by many others (eg. Lavery & Henry 1986; Couch & Sharples 1987; Ellingson et al. 2001), the fraction of blue galaxies in clusters increases with redshift, the so called Butcher-Oemler effect. Despite this, the fraction of star forming galaxies in groups and clusters is still lower than the coeval field fraction at least to $z=1$ (Wilman et al. 2005; Gerke et al. 2007; Balogh et al. 2009). The need to explain the Butcher-Oemler effect, as well as the local properties of galaxy clusters provides important constraints for the nature of the transformation mechanism. Essentially, if the transformation mechanism only occurs in very massive clusters, then the fraction of blue galaxies is simply the fraction of galaxies which have fallen into the cluster within the time scale of transformation.

The time scale for transformation of galaxy properties to occur is a significant uncertainty in attempting to link the growth of structure to the Butcher-Oemler effect. Previous attempts using cluster assembly histories adopted relatively short time scales of ~ 1 Gyr and, while complicated by uncertain cosmological parameters, showed that a direct infall model alone did not produce enough evolution in the blue fraction (Bower 1991; Kauffmann 1995). Kodama & Bower (2001) combined the evolving star formation properties of field galaxies with a cluster infall model to

successfully reproduced the scatter in the red sequence of low redshift clusters. Similarly, Ellingson et al. (2001) found that the radial distribution of early type galaxies in galaxy clusters at two redshift epochs could best be explained if the galaxy infall into clusters decreased by a factor of ~ 3 between $z > 0.8$ and $z \sim 0.5$.

In this paper, we examine the *galaxy* assembly properties of groups and clusters over a wide mass range and at four redshift epochs. We investigate the mass of halos through which groups and clusters gain their galaxies and the extent to which preprocessing in the group environment is important at four redshift epochs. By making simple assumptions, we investigate the predictions for the fraction of galaxies in groups and clusters which are “environmentally affected” for a range of relevant timescales and the halo mass thresholds which those effects begin. Using these models we try to gain insight into the dominant physical processes necessary to reproduce observations of group and cluster galaxies, as well make predictions for future observations. In §2, we present the details of our simulated clusters and some of their properties and present our results in §3. We discuss these results and conclude in §4. In this paper, we assume a cosmology with $\Omega_m = 0.25$, $\Omega_\Lambda = 0.75$, $\sigma_8 = 0.9$ and $H_0 = 100h$ km s $^{-1}$ Mpc $^{-1}$ unless mentioned otherwise.

2 SIMULATIONS

To interpret observations of galaxy properties as a function of environment, we need to know the accretion history of those galaxies; as shown by B09 this can be subtly different from the total mass assembly history. But galaxy formation has proven to be a difficult problem, and it is not clear, given that the dark matter halo mass function has a very different shape from the galaxy luminosity function, if the approach of B09 of simply associating subhalos with galaxies includes all of the relevant physics. At the least, this approach does not allow for the robust identification of the stellar masses of galaxies. Unfortunately, an obvious alternative — the direct simulation of the baryonic processes of galaxies — is difficult on the scale of the cosmological volumes needed to study large samples of groups and clusters.

Semi-analytic galaxy formation models provide a good tool to encapsulate the essential physical processes of gas cooling, star formation and feedback (e.g. White & Frenk 1991; Kauffmann et al. 1993; Somerville & Primack 1999; Croton et al. 2006; Bower et al. 2006). Dark matter simulations, on which modern semi-analytic models are based, are now large enough to allow the study of the growth of the groups and clusters over a wide range of redshifts. We make use of one such semi-analytic model by Font et al. (2008, hereafter F08), which is a recent modification to the Durham semi-analytic model (GALFORM) of Bower et al. (2006). The basic prescriptions for gas cooling and star formation in the GALFORM model was laid out by Cole et al. (2000), and subsequently modified for modern cosmological parameters by Benson et al. (2003). The model of Bower et al. (2006) introduced a method for parameterizing the effect of AGN feedback on the gas in massive galaxies to correct for the “overcooling” problem.

The Bower et al. (2006) model, as in essentially all previous semi-analytic models, implements a relatively simple treatment of environmental effects, in which the hot gas reservoirs of galaxies are removed upon becoming a satellite galaxy. Many authors have since shown that this approach produces an unphysically high fraction of red galaxies in groups and clusters (Weinmann et al. 2006; Baldry et al. 2006; Gilbank & Balogh 2008). The F08 model implements a more realistic “strangulation” model in which the hot

gas halo of galaxies falling into more massive halos are removed according to a prescription of McCarthy et al. (2008b). However, a careful examination of cluster and group data with this model at a range of redshifts reveal that there are important discrepancies. In particular, the model overpopulates the green valley between the blue cloud and red sequence Balogh et al. (2009, McGee et al., in prep.). We emphasize that despite this difficulty in reproducing galaxy colours, the stellar masses of galaxies in the F08 and Bower et al. models are much better understood. In particular, the Bower et al. model reproduces the observed evolution of the stellar mass function out to at least $z=5$.

In this paper, our analysis relies primarily on the GALFORM prediction of the stellar mass function of galaxies in different environments. This is insensitive to the problem noted above, as the star formation rate of galaxies declines rapidly with redshift, so the bulk of a galaxy's stellar mass is already in place before it ever becomes a satellite. Thus, the details of the strangulation procedure adopted in GALFORM are unimportant for our analysis and, indeed, all our conclusions are independent of the choice of either the Bower et al. model or the F08. model.

2.1 Cluster and group sample

The F08 model, from which our simulated galaxy clusters and groups are drawn, is based on merger trees derived from the dark matter Millennium simulation (Springel et al. 2005), a Λ CDM cosmological box with $500/h$ Mpc sides. The Millennium simulation uses GADGET2 (Springel 2005), a TREE-PM N-body code, and an initial power spectrum calculated using CMBFAST (Seljak & Zaldarriaga 1996). The merger trees are generated as described in Helly et al. (2003) and Harker et al. (2006), and are complete down to halos which host $\sim 10^8 h^{-1} M_\odot$ galaxies. In this paper, we are principally concerned with selecting samples of galaxies which are observationally accessible, and thus specify a single fixed stellar mass cut of $M > 10^9 h^{-1} M_\odot$, much higher than the completeness limit.

We analyze all the groups and clusters in the F08 model more massive than $M = 10^{12.9} h^{-1} M_\odot$ at four redshift epochs ($z=0, 0.5, 1$ and 1.5). The key properties of the cluster samples are shown in Table 1. In particular, we show the number of clusters, and the average number of galaxies with stellar masses above $M = 10^9 h^{-1} M_\odot$ at the epoch of observation, in each of the mass bins which will be used in the remainder of the paper.

In Figure 1, we present the cumulative distribution of galaxies which reside within the virial radius of host halos of a given mass. We plot this for four stellar mass ranges at $z=0$. In the F08 model, $\sim 50\%$ of $z = 0 L_*$ galaxies are in host halos with masses above $10^{12.5} h^{-1} M_\odot$. This compares very well with observational results: Berlind et al. (2006) found that $\sim 56\%$ of $M_r < -20.5$ galaxies in the SDSS are linked to groups containing at least one other member, a result that is completely consistent with independent analysis using the 2dFGRS Eke et al.. We also see that 25% of L_* galaxies are in relatively large groups or clusters with halo masses above $10^{13} h^{-1} M_\odot$. This is much larger than the $\sim 10\%$ claimed by B09, likely a result of the way they assign galaxies to subhalos, as discussed further in §3.6. In particular, B09 assign a galaxy to a subhalo if the subhalo mass is $> 10^{11.5} h^{-1} M_\odot$ when it is accreted into a more massive host. However, the mass in a subhalo begins to be tidally stripped significantly before reaching the virial radius of a more massive host, even without significantly disturbing the galaxy within (Natarajan et al. 2007).

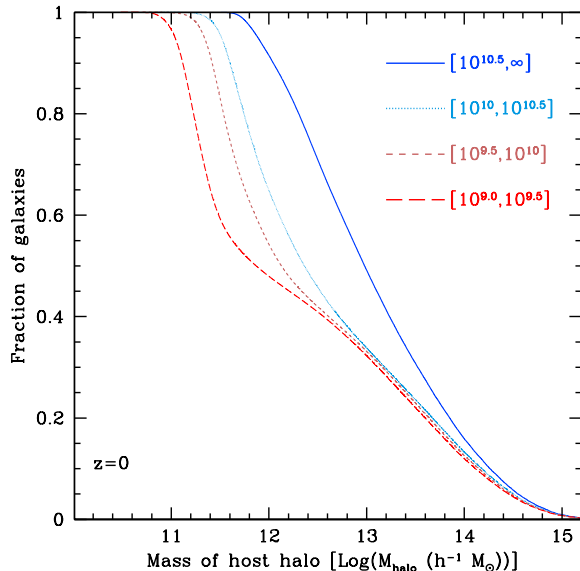


Figure 1. The cumulative distribution of the host halo mass of galaxies at $z=0$. The distribution is shown for four ranges in the galaxy's stellar mass at $z = 0$, shown in the upper right corner in units of $h^{-1} M_\odot$.

3 RESULTS

We now look in detail at how the cluster galaxies end up in the clusters, and what insights this might give into the processes which might affect those galaxies.

3.1 Cluster and group accretion history

Galaxies which have been in massive halos prior to joining the final environment may have been environmentally pre-processed. Thus, we begin by examining the host halo masses of galaxies just prior to their accretion into the final group or cluster halo. To achieve this, we trace the most massive progenitor of every galaxy, back through each snapshot in the simulation. We record the halo mass of this progenitor in the timestep just before it becomes a member of the final cluster, which defines its environment at the time of accretion.

We show the full accretion histories for all the cluster mass bins, in each of the four redshift epochs, in the Appendix. Here we will examine the most important insights which can be drawn from those accretion histories. Figure 2 shows the fraction of galaxies in the final cluster which were accreted through haloes at least as massive as $10^{13} h^{-1} M_\odot$ (large groups). We show this as a function of the final cluster mass for each of four redshift epochs. We first consider relatively low-mass clusters, with $M \sim 10^{14.2} M_\odot$ at $z=0$. We find that 32 per cent of galaxies in these clusters were accreted through such group-sized halos. This is somewhat higher than the 24 per cent found by B09; the small difference can be related to the difference in the way haloes are populated with galaxies, as we discuss in § 3.6.

However, such clusters are fairly poor systems; they are less massive than all 16 clusters observed extensively by the CNOC1 collaboration (Carlberg et al. 1996), and an order of magnitude smaller than the nearby Coma cluster ($M_{200} = 1.88^{+0.65}_{-0.56} \times 10^{15} h^{-1} M_\odot$, (Kubo et al. 2007)). Figure 2 shows that the fraction of galaxies which are accreted through group sized halos is strongly

Redshift	Number of clusters	Mass range Log($h^{-1} M_{\odot}$)	Median mass Log($h^{-1} M_{\odot}$)	Average number of galaxies per cluster
0	40	15.0-15.6	15.14	1161
	189	14.7-15.0	14.82	569
	673	14.4-14.7	14.53	297
	1822	14.1-14.4	14.24	156
	4404	13.8-14.1	13.94	78
	9325	13.5-13.8	13.64	41
	18730	13.2-13.5	13.34	20
	36265	12.9-13.2	13.04	10
0.5	4	15.0-15.6	15.16	1161
	29	14.7-15.0	14.79	536
	212	14.4-14.7	14.51	289
	786	14.1-14.4	14.23	156
	2471	13.8-14.1	13.93	80
	6325	13.5-13.8	13.68	42
	14440	13.2-13.5	13.34	22
	30124	12.9-13.2	13.04	11
1.0	0	15.0-15.6	–	–
	3	14.7-15.0	14.82	532
	40	14.4-14.7	14.51	252
	275	14.1-14.4	14.22	137
	1134	13.8-14.1	13.92	72
	3643	13.5-13.8	13.63	38
	9820	13.2-13.5	13.34	21
	23388	12.9-13.2	13.04	11
1.5	0	15.0-15.6	–	–
	1	14.7-15.0	14.81	381
	2	14.4-14.7	14.41	178
	55	14.1-14.4	14.19	119
	322	13.8-14.1	13.92	66
	1528	13.5-13.8	13.62	35
	5465	13.2-13.5	13.33	19
	15134	12.9-13.2	13.03	10

Table 1. Properties of the cluster sample derived from Font et al. (2008). The first column lists the redshift snapshot from which the clusters were selected and the second column gives the total number of clusters used for analysis in each bin. Columns 3 and 4 list the cluster halo mass range and median mass of clusters in that range. We use these halo mass bins extensively in the rest of the paper. Column 5 lists the average number of galaxies per cluster with stellar masses above $M = 10^9 h^{-1} M_{\odot}$ at the epoch of observation.

dependent on the mass of the final halo. This is because massive haloes are not surrounded by an average patch of the universe, but tend to be strongly clustered with other massive halos (eg. Kaiser 1984). At $z=0$, we see that 45 % of galaxies accreted into a cluster of Coma’s mass have been accreted from haloes with $M > 10^{13} h^{-1} M_{\odot}$. This suggests that pre-processing in group environments before cluster accretion may be significant. Interestingly, the fraction of galaxies accreted through massive haloes has only a weak dependence on the redshift of observation of the cluster. In other words, a Coma-sized cluster at $z=0.5$ would accrete 40 % of its galaxies from $M > 10^{13} h^{-1} M_{\odot}$ halos. The galaxy assembly histories are remarkably similar, with the dominant difference being simply that Coma-sized clusters do not exist in the relatively small volume of the Millennium simulation at $z = 1.0$ or 1.5 .

In Figure 3, we show the fraction of stellar mass which is accreted through halos at least as massive as $10^{13} h^{-1} M_{\odot}$. This figure is quite similar to Figure 2. However, notice that the fraction of *stellar mass* accreted by the most massive clusters through groups is larger than the fraction of *galaxies* accreted through such systems. Indeed, the stellar mass accretion history closely matches the expected behavior of the dark matter accretion. The extended

Press Schechter formalism and n-body simulations of dark matter roughly agree that ~ 30 % of the mass of a halo is accreted from halos with masses a tenth the mass of the final halo (Bond et al. 1991; Bower 1991; Lacey & Cole 1993; Stewart et al. 2008). We find this same fraction for all our stellar mass accretion histories, while the fraction of galaxies accreted is smaller at high cluster mass. This implies there are fundamental differences in how galaxies are accreted as a function of their stellar mass. This is illustrated in Figure 4, where we show the accretion histories of galaxies which end up in a $M = 10^{15.0} h^{-1} M_{\odot}$ cluster at $z=0$, binned by their final stellar mass. There is a large difference in the masses of the host halos prior to accretion for low and high mass galaxies. While ~ 52 % of the most massive galaxies are accumulated from haloes with $M > 10^{13} h^{-1} M_{\odot}$, this is only the case for ~ 45 % of the least massive galaxies we consider. This discrepancy is much larger if we consider accretion through poorer groups, with $M > 10^{12} h^{-1} M_{\odot}$. The more massive galaxies are more likely to have been accumulated from group mass halos, and thus more likely to have been pre-processed prior to accretion into a cluster.

Now that we have seen that the degree of group pre-processing depends on both the stellar mass of the galaxy and the mass

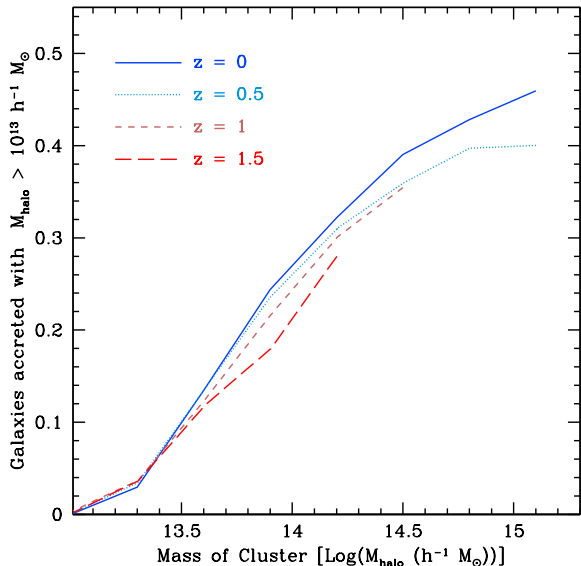


Figure 2. The fraction of cluster galaxies which were accreted into the final cluster halo as a member of a halo with $M > 10^{13} h^{-1} M_{\odot}$. This is shown as a function of the final cluster mass at the epoch of observation, for four redshifts. All cluster galaxies have final stellar masses of $M > 10^9 M_{\odot}$. The mass range bins were defined in Table 1, and are shown for all bins containing more than two clusters.

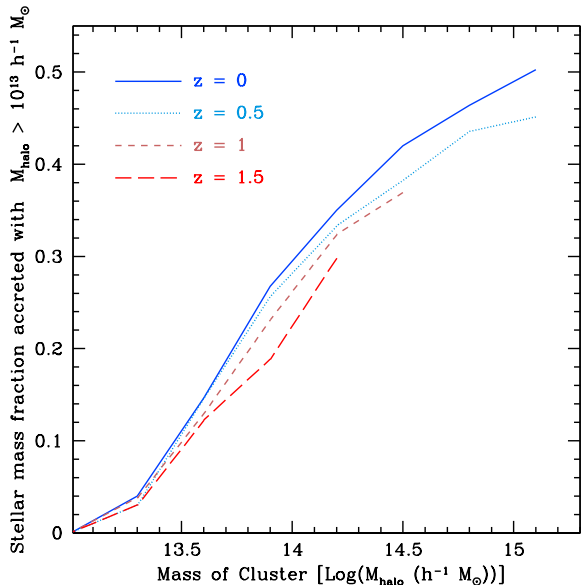


Figure 3. As Figure 2, but showing the fraction of accreted *stellar mass* which resides in a $M > 10^{13} h^{-1} M_{\odot}$ halo at the time of accretion.

of the final cluster, we would like to examine how this varies as a function of redshift. In Figure 5 we show the fraction of cluster galaxies which were accreted into the final cluster halo as a member of a halo with $M > 10^{13} h^{-1} M_{\odot}$ halo. This is broken up into three bins, which represent the redshift at the time of the galaxy's accretion into the cluster. From this we see that the degree of pre-processing is significantly dependent on the time the galaxies were accreted. Galaxies which are accreted recently into the cluster are

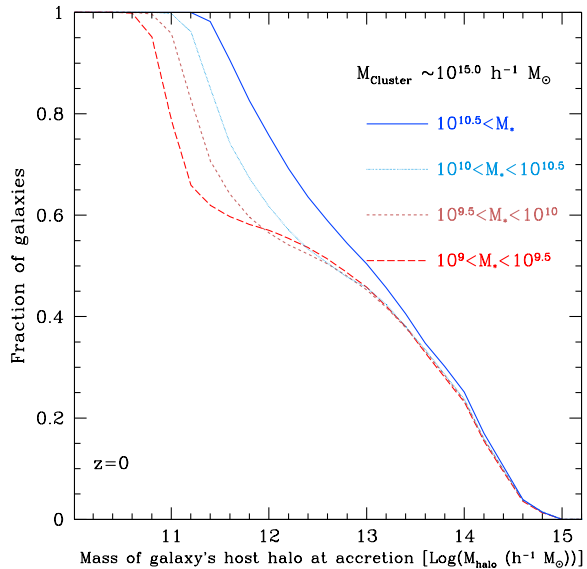


Figure 4. The cumulative distribution of accreted cluster galaxies as a function of host halo mass at the time of accretion into the final cluster. The distribution is shown in three stellar mass bins at $z=0$, for a final cluster with $M = 10^{15} h^{-1} M_{\odot}$.

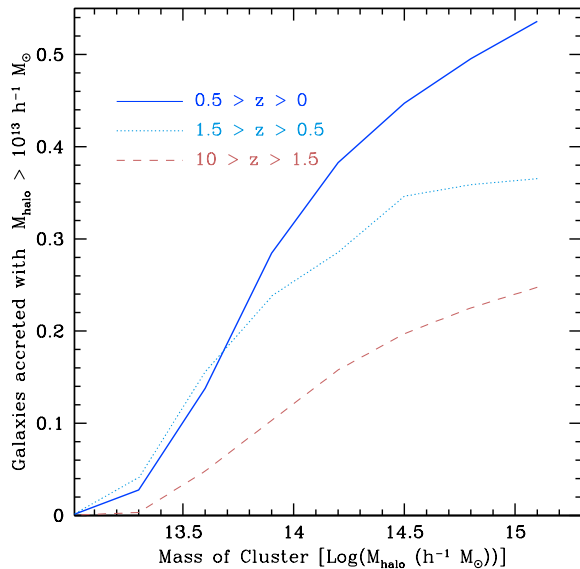


Figure 5. The fraction of cluster galaxies which were accreted into the final cluster halo as a member of a $10^{13} h^{-1} M_{\odot}$ halo or greater. This is shown as a function of the final cluster mass $z=0$ and for three bins in accretion redshift. All cluster galaxies have final stellar masses of $M > 10^9 M_{\odot}$.

more likely to have been in a group environment than ones accreted into the cluster at high redshift. In particular, since $z = 0.5$ the most massive clusters today have accreted most of their new galaxies via infalling groups.

3.2 Cluster and group assembly histories

We have seen that the accretion history of clusters varies with final cluster mass, is a function of the stellar mass of the accreted galaxy and is dependent on the redshift of accretion. However, this does not address the state of the cluster itself. The importance of pre-processing depends not only on the accretion history but also on the amount of time the main cluster progenitor itself had the mass of a group.

Therefore, to get a complete picture of the assembly of galaxy clusters and groups and the halo masses which are important for the properties of their galaxies we present Figure 6. This shows the distribution of halo masses in which the most massive progenitors of final $z=0$ cluster galaxies reside, as a function of lookback time and for four bins of final $z=0$ cluster mass. The panels in Figure 6 show distinctly different assembly histories for very massive clusters, smallish clusters, and groups. In particular, the relative importance of the group environment varies tremendously for these three types of structures. The most massive cluster never has more than 17% of galaxies in group sized halos ($10^{13} h^{-1} M_{\odot} < M_{\text{halo}} < 10^{14} h^{-1} M_{\odot}$) while as many as 44% of the galaxies in a $M \sim 10^{14.2} h^{-1} M_{\odot}$ cluster today have spent some time within such haloes in the past. In fact, for a period of 2 Gyrs, groups are the most common environment of the galaxy progenitors; this is because during this time the main cluster progenitor itself has the mass of a group. Thus, considering only the haloes of galaxies prior to accretion into the main cluster may underestimate the role of the group environment, as already noted by B09.

Given the distinctly different assembly histories of these clusters and massive groups, it is perhaps surprising that observations of large samples of galaxy clusters in the local universe show that the fraction of red galaxies is approximately constant in clusters more massive than $10^{13.8} h^{-1} M_{\odot}$ (Hansen et al. 2007). Therefore, it is useful to look for some common trait in the assembly histories of clusters which may point to the reason for this uniformity. It is interesting that the population of ‘isolated’ galaxies, those in $10^{11} h^{-1} M_{\odot} < M_{\text{halo}} < 10^{12} h^{-1} M_{\odot}$, shows a similar distribution in the four different panels. At a lookback time of 10 Gyrs, $\sim 55\%$ of cluster galaxy progenitors were in this halo mass regime, and that percentage has declined at a nearly constant rate of 5–6% per Gyr until the current epoch, regardless of the final cluster mass. In other words, the distribution of galaxies not in ‘isolated’ halos is similar regardless of final cluster mass, and supports the hypothesis that the galaxy transformation mechanism begins to occur as galaxies leave their ‘isolated’ halos.

Finally, we examine the assembly histories of galaxy clusters of a given mass at each redshift epoch. In Figure 7 we show the distributions of halo masses for the most massive progenitors of $10^{14.5} h^{-1} M_{\odot}$ cluster galaxies as a function of lookback time at all four redshift epochs. While the final cluster mass is the same (at each epoch), the higher redshift clusters must assemble their mass more quickly and thus their galaxies have not been in massive halos for as long. For instance, 5 Gyrs prior to the observation epoch, $\sim 50\%$ of $z=0$ galaxies were in $10^{14} M_{\odot} h^{-1}$ haloes, while none of the $z=1$ or $z=1.5$ cluster galaxies were even in $10^{13} h^{-1} M_{\odot}$ haloes yet. Environmental processes have had a much longer timescale over which to affect low redshift groups and clusters than higher redshift ones.

There are two interesting points when comparing Figure 7 with Figure 6. First, we see that the maximum fraction of galaxies in each halo mass bin is the same in clusters of the same final mass but seen at different redshifts. For instance, the maximum fraction

of galaxies which reside in halos of $10^{13} h^{-1} M_{\odot} < M_{\text{halo}} < 10^{14} h^{-1} M_{\odot}$ at any time is 40% regardless of the redshift epoch. The lookback time at which these maximum fractions occur varies significantly with redshift, but it would appear their path through the hierarchy is similar. Essentially, clusters of fixed mass at different redshift epochs have assembly histories which become more stretched out at lower redshift. The assembly histories would look almost identical if the lookback time was divided by the age of the universe at that redshift epoch. This result was hinted at in Figure 2, which showed that the fraction of galaxies accreted through massive haloes was approximately the same at all redshift epochs for a cluster of given mass.

This leads to the second interesting observation to be made from Figure 7. The rate at which galaxies leave their ‘isolated’ halos increases significantly with redshift. At $z=0$, as before, for the 10 Gyrs prior to observation the fraction of galaxies in halos of $10^{11} h^{-1} M_{\odot} < M_{\text{halo}} < 10^{12} h^{-1} M_{\odot}$ decreases by about 5–6% per Gyr, while 10% (15%) [20%] of galaxies leave their ‘isolated’ halos per Gyr at a constant rate for 5(3.5)[2.5] Gyrs prior to observation at $z=0.5(1)[1.5]$. Therefore, the accretion rate of galaxies from isolated environments into groups and clusters is higher at higher redshift. Again, this result is a direct result of the reduced time between the epoch of observation and the beginning of the universe. The assembly histories at higher redshift are just compressed, leading to a higher accretion rate, even though the total number accreted from isolated environments is constant at each epoch of observation. The effect this has on the galaxy properties of galaxy clusters as a function of redshift will be discussed in the following section.

3.3 Cluster to cluster variation in environmental effects

We have established the galaxy accretion history and galaxy assembly history of galaxy clusters at a range of epochs. We would now like to assess how these galaxy histories affect the final properties of galaxies at each redshift epoch. To this end, we examine the fraction of galaxies in each cluster, which have been within dense environments long enough to expect that environmental effects might be important. By examining the fraction of environmentally affected galaxies in each cluster, we can quantify both the total numbers of affected galaxies, and their variation from cluster to cluster.

In a simple way, we can parametrize the length of time it takes for a galaxy to display an environmental effect, T_{trunc} , after falling into a halo with a mass above a characteristic mass threshold, M_{trunc} . Although it is not obvious that there is a single main physical mechanism which causes the environmental effects displayed in both groups and clusters, we explore the predictions of such a model and discuss the limitations of this approach in the following section.

Given this model we can explore how varying the truncation time, T_{trunc} , and the characteristic mass threshold, M_{trunc} , alters the implied environmental effects on galaxies. In Figure 8, we show the predicted average fraction of galaxies in each cluster which are subject to environmental effects in our simple model; the distribution of this fraction is reflected in the four contour lines marking the 10, 33, 67 and 90 percentiles. Here we fix the truncation time, T_{trunc} , to be 3 Gyr and allow the characteristic mass threshold, M_{trunc} , to vary from $10^{12} h^{-1} M_{\odot}$ to $10^{14} M_{\odot}$. In other words, in this figure, a galaxy has felt an ‘environmental effect’ if it has been within a halo of mass $M \geq M_{\text{trunc}}$ for at least 3 Gyrs. In addition, we allow a fourth category, in which the expression of an environ-

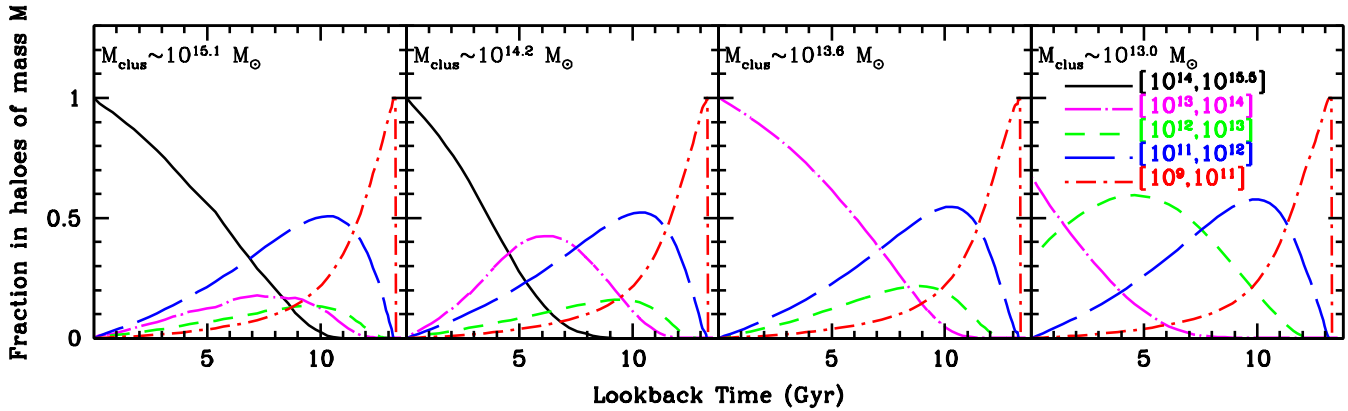


Figure 6. The fraction of galaxies residing in $z=0$ clusters that are found in haloes of mass M at a previous time t . We only consider the most massive progenitor of each cluster galaxy. Each curve shows a range of M , indicated by the legend, in units of $h^{-1} M_{\odot}$. Each panel represents clusters of different final masses, as indicated in the top-left corner. Note that the curve corresponding to haloes with $10^{11} < M/h^{-1} M_{\odot} < 10^{12}$ is very similar in all cases, indicating that the accretion rate of “isolated” galaxies is roughly independent of final cluster mass.

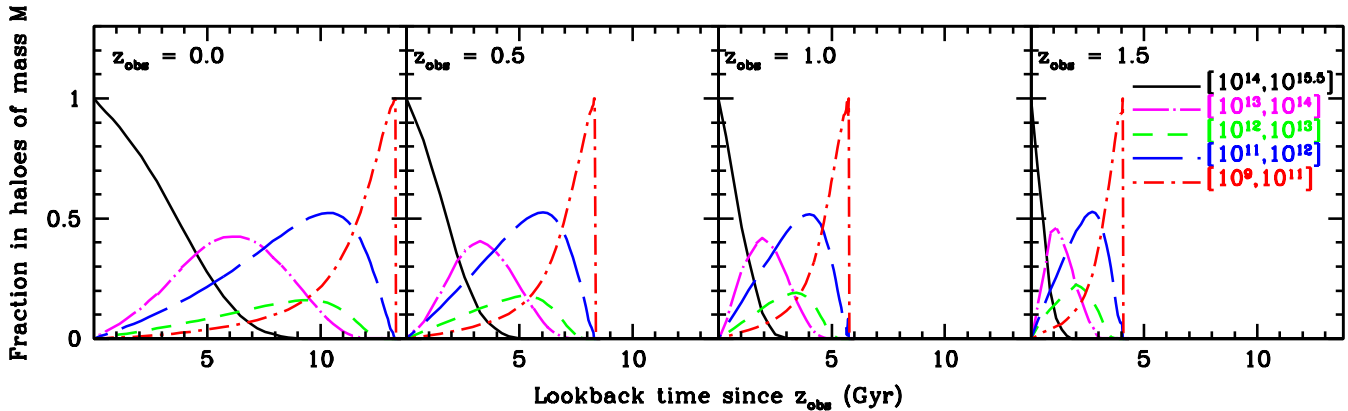


Figure 7. As in Figure 6, but for a cluster of mass $10^{14.5} (h^{-1} M_{\odot})$ observed at four redshift epochs as indicated at the top of each panel. Clusters of a given mass at higher redshift must assemble their mass more quickly, and thus the time available for pre-processing through group-sized haloes is decreased.

mental effect occurs 3 Gyrs after the galaxy has become a satellite galaxy in a larger dark matter halo, regardless of its mass.

This figure has some noteworthy features. First, for massive clusters ($M > 10^{14.5} h^{-1} M_{\odot}$) at $z=0$, the mean number of environmentally affected galaxies in this model is similar (~ 80 -85 %) regardless of M_{trunc} . The implication of this for low redshift observational studies is that it is difficult to discern the value of the characteristic mass threshold by observing systems above that mass threshold. This highlights the importance of studies of low mass galaxy groups. Observations at low and intermediate redshift show that group galaxies with a given stellar mass have properties distinct from the average field galaxy; if our simple model of environment-driven transformation is correct, this indicates a characteristic mass threshold of at least this scale ($M \approx 10^{12.5} - 10^{13} h^{-1} M_{\odot}$) (Wilman et al. 2005; Weinmann et al. 2006).

Indeed, as previously mentioned, low redshift observations show that the fraction of red galaxies in clusters is essentially uniform, for clusters with $M > 10^{13.8} h^{-1} M_{\odot}$ (Hansen et al. 2007). Given this, it is also worth noting that in Figure 8, our model also produces a strikingly flat fraction of environmentally affected galaxies per cluster as a function of cluster mass. This is a direct result of the behavior noted in Figure 6, that the fraction of galaxies infalling from isolated haloes is independent of halo mass.

Although it may be difficult to use the average properties of massive clusters at a given epoch to discern the characteristic mass threshold, one possible method would be to observe the variation in their properties. The predicted scatter in the fraction of environmentally affected galaxies per cluster is quite small (~ 5 %) for $10^{14.5} h^{-1} M_{\odot}$ clusters at $z=0$ when $M_{\text{trunc}} = 10^{12} h^{-1} M_{\odot}$, but close to 40 % when $M_{\text{trunc}} = 10^{14} h^{-1} M_{\odot}$. The scatter in, for instance, the fraction of early type galaxies or optical line emitting galaxies in clusters at $z=0$ is much smaller than 40 % (Dressler 1980; Poggianti et al. 2006; Finn et al. 2008). We will examine the scatter in red fractions of galaxies in clusters at $z=0$ in a future paper. Unfortunately, the scatter at $z=0$ of a model where $M_{\text{trunc}} = 10^{12} h^{-1} M_{\odot}$ is not that different from a model where $M_{\text{trunc}} = 10^{13} h^{-1} M_{\odot}$. However, notice that the scatter in these two models becomes more significant at $z > 0$. Intriguingly, Dressler et al. (1997) showed that, while the morphology-density relation was equally strong in all clusters at low redshift, the relation was stronger in centrally-concentrated clusters than irregular clusters at $z \sim 0.5$.¹ In effect, this suggests that the scatter in the fraction of environmentally affected galaxies of each cluster is sig-

¹ While the Dressler et al. results, and many intermediate redshift results, have limiting stellar mass on the order of $10^{10} h^{-1} M_{\odot}$ compared with our

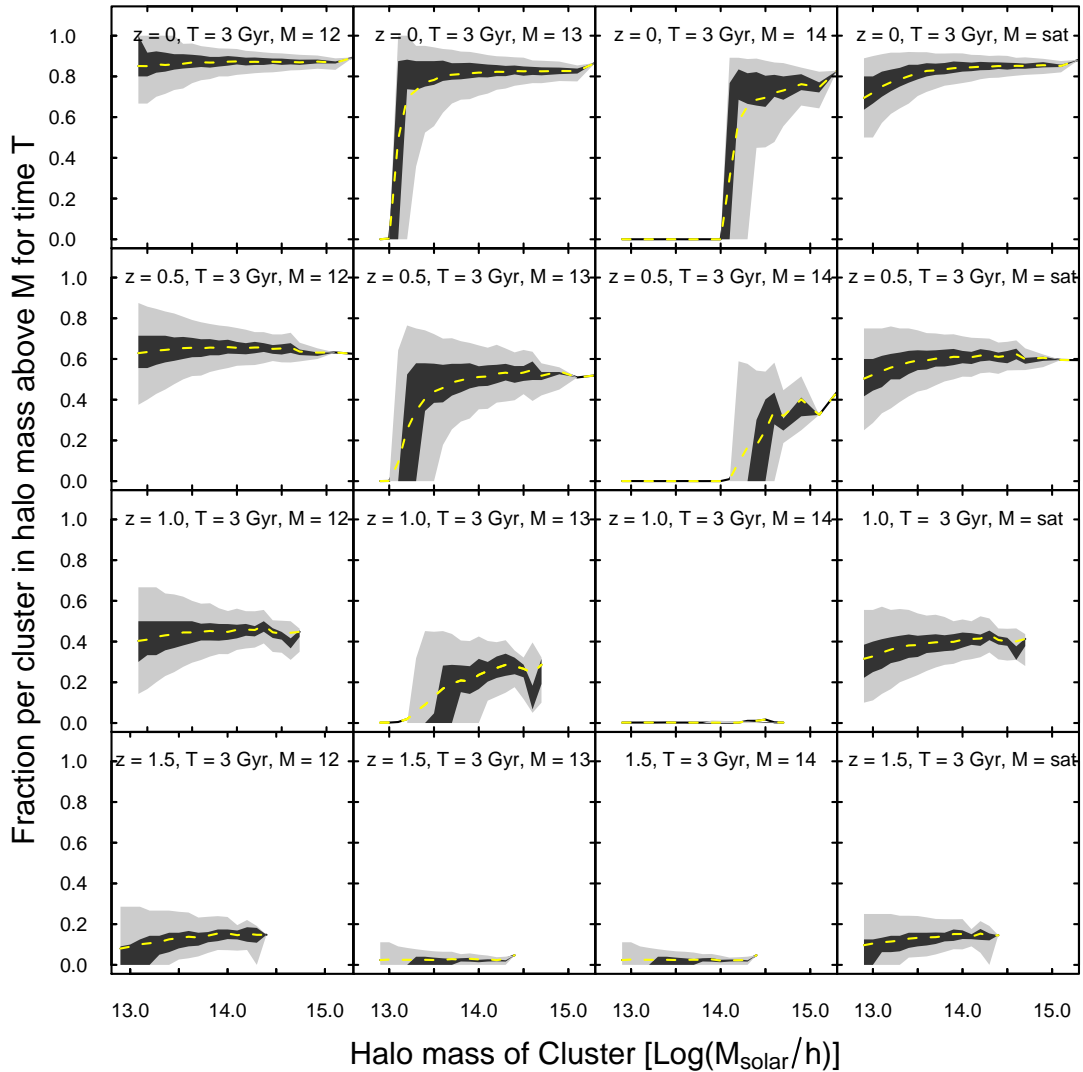


Figure 8. The fraction of cluster galaxies with $M > 10^9 h^{-1} M_{\odot}$ that have resided within a halo of mass $M \geq M_{\text{trunc}}$ for a time $t \geq T_{\text{trunc}}$ is shown as a function of final cluster mass. We interpret this as the fraction of “environmentally-affected” population in our simple model. The panels contain four contour lines marking the 10, 33, 67 and 90 percentiles of the distribution in this fraction, while the dashed yellow line represents the average. The truncation time is fixed at $T_{\text{trunc}} = 3$ Gyr, and each row shows a different assumption for M_{trunc} , as indicated. Different rows correspond to clusters at a different redshift, as indicated.

nificant at $z \sim 0.5$. Although not definitive, this may point to a characteristic mass threshold which is somewhat larger than $10^{12} h^{-1} M_{\odot}$, given that scatter in that model is still quite small at $z=0.5$ ($\sim 13\%$ at $10^{14.5} h^{-1} M_{\odot}$). Notice that a model where the environmental effects begin to occur when a galaxy becomes a satellite behaves very similarly to a model with $M_{\text{trunc}} = 10^{12} h^{-1} M_{\odot}$. We discuss this similarity further in §3.7.

Examining the redshift evolution of any of the given models shows that they all predict a significant Butcher-Oemler effect. That is, they predict that there are fewer environmentally affected galax-

ies in clusters with increasing redshift. In particular, by $z = 1.5$ all of the models predict a very small or non-existent fraction of environmentally affected galaxies. Indeed, the $10^{14} h^{-1} M_{\odot}$ model leads to the prediction that, by $z = 1$, no galaxies will be environmentally affected.

Our choice of $T_{\text{trunc}} = 3$ Gyrs in the models presented above is ad hoc, and we would like to quantify how changing the timescale effects the predictions. In Figure 9, we explore a model in which the characteristic halo mass, M_{trunc} , is kept fixed at $10^{12} h^{-1} M_{\odot}$, and allow T_{trunc} to vary from 1 Gyr to 4 Gyrs. We show the fraction of environmentally affected galaxies for each of the four redshift epochs of our clusters. Although M_{trunc} is held constant, we note that the results and our interpretation are similar for any choice

limit of $10^9 h^{-1} M_{\odot}$, we have verified that the scatter in the cluster red fractions is constant with a limiting mass change to $10^{10} h^{-1} M_{\odot}$.

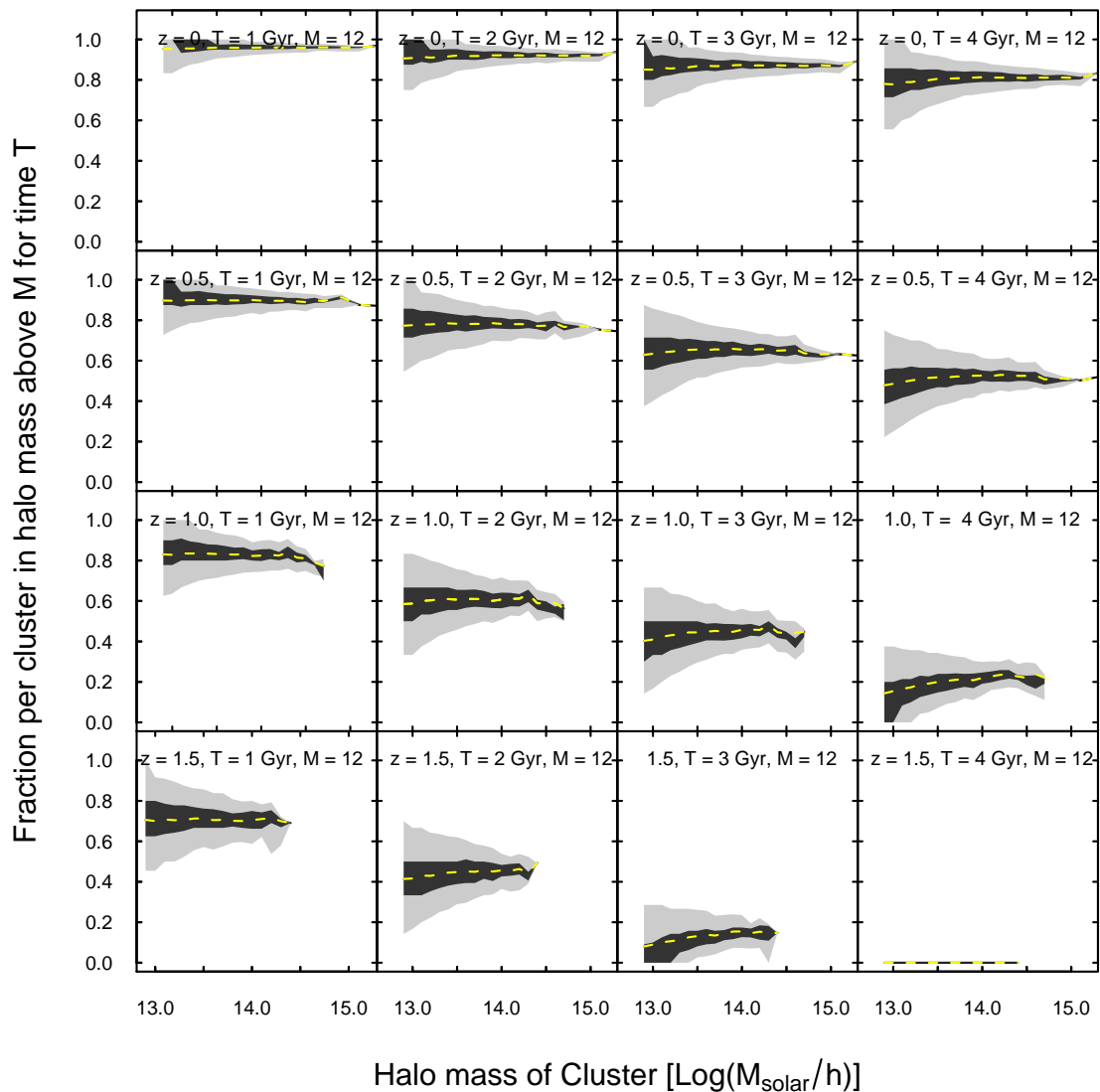


Figure 9. As Figure 8, but where the characteristic halo mass threshold is fixed at $M_{\text{trunc}} = 10^{12} h^{-1} M_{\odot}$, and the truncation times T_{trunc} are varied along rows of the figure, from 1–4 Gyr as indicated.

of M_{trunc} within the range $10^{12} - 10^{13} h^{-1} M_{\odot}$, which seems the most likely value given the arguments above.

Similarly to Figure 8, for each T_{trunc} , we see a significant Butcher-Oemler effect, such that clusters at higher redshift have fewer galaxies affected by environmental processes. However, the size of the effect even between $z = 0$ and $z = 0.5$ is dramatically altered by the choice of time scale. With a short timescale of only 1 Gyr, the fraction of environmentally-affected galaxies evolves little, from $\sim 85\%$ at $z = 0.5$ to $\sim 95\%$ today. On the other hand, a long timescale of $T_{\text{trunc}} = 4$ Gyr results in a much stronger evolution over this redshift range, from 50% to 80%. Compare this evolution with that observed in the red fraction of cluster galaxies, which indicate an evolution of $\sim 25\%$ over a similar redshift range, from 0.9 at $z=0.2$ to 0.65 at $z=0.5$ (Ellingson et al. 2001). This seems to indicate that a relatively long time scale for the expression of environmental effects (> 2 Gyr) would be required to match this quick

evolution. A similar timescale is necessary to explain the radial gradient of passive galaxies in galaxy clusters (Ellingson et al. 2001; Balogh et al. 2000).

The predicted scatter from cluster to cluster is also noteworthy. Recall that in Figure 8 we saw that the scatter was sensitive to the characteristic halo mass used. In this plot, for the majority of the time, the scatter is similar at each redshift regardless of the timescale for truncation. This strengthens our previous argument that a well-defined measure of the scatter in cluster properties at a given redshift could allow one to discern the characteristic halo mass for truncation.

We have provided strong evidence, which we summarize in §3.5, that the dominant environmental processes at work in galaxy groups and clusters begin to become effective at a halo mass scale of $10^{12} - 10^{13} h^{-1} M_{\odot}$, and are active for a timescale of at least a few Gyrs. Given these constraints, we see that figure 9 predicts that

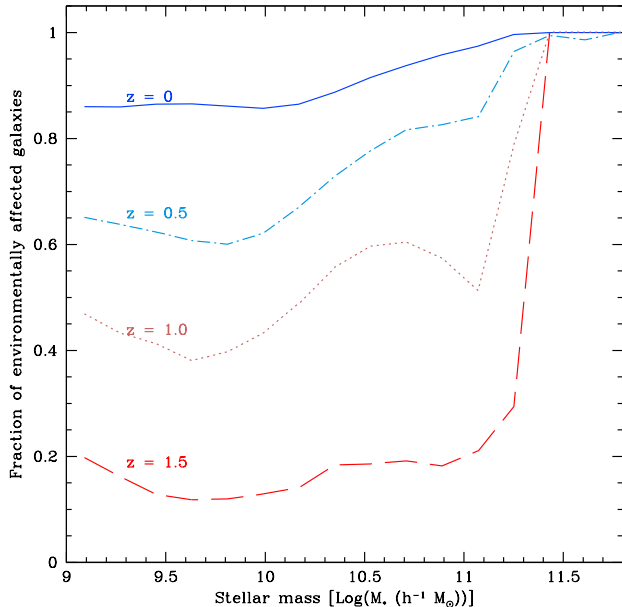


Figure 10. The fraction of environmentally affected galaxies in clusters at all four redshift epochs as a function of galaxy stellar mass. Cluster galaxies have host halo masses greater than $10^{14} h^{-1} M_{\odot}$ at the epoch of observation. This model assumes $M_{\text{trunc}}=10^{12} h^{-1} M_{\odot}$ and $T_{\text{trunc}}=3$ Gyrs as in Figure 8.

by $z=1.5$ there should be little to no environmental effect on galaxies. Remarkably, this prediction has some observational evidence to suggest it is correct. Cooper et al. (2007) showed, using galaxies selected from the DEEP2 redshift survey, that the red fraction only weakly correlates with overdensity at $z \sim 1.3$. While the comparison to our predictions is complicated because the Cooper et al. sample only includes massive galaxies, this is not a trivial agreement; in fact, assuming the timescale was 1 Gyr, this would lead us to predict that 70 % of galaxies at $z=1.5$ are still environmentally affected. This fraction would be even higher when we used the same limiting stellar mass as Cooper et al., as is discussed in the next section. Additionally, the DEEP2 survey is complicated by their rest frame blue magnitude limit which causes them to naturally detect fewer and fewer red galaxies at higher redshifts. Further, DEEP2 does not cover a wide enough area to have massive clusters within it, so targeted, stellar mass limited studies of the extreme cluster environments are still needed at this redshift to quantify the size of the environmental effects. Although, given our results, they may be difficult to find using the popular and efficient red sequence method (Gladders & Yee 2000; Lu et al. 2009).

3.4 Stellar mass dependence of environmental effects

Observations suggest that the fraction of galaxies which are passive or red, depends greatly on their own stellar mass (Baldry et al. 2006; Haines et al. 2006). It is thought that this is at least partially due to secular influences, ie. AGN feedback, which primarily occur in massive galaxies (Kauffmann et al. 2003). We can use our simple model for environmental effects to examine the fraction of cluster galaxies (those with $M_{\text{halo}} > 10^{14} h^{-1} M_{\odot}$) which may also be subject to environmental effects. This is presented in Figure 10 for a model which has $M_{\text{trunc}}=10^{12} h^{-1} M_{\odot}$ and $T_{\text{trunc}}=3$ Gyr at all four redshift epochs.

The fraction of environmentally affected galaxies is a strong

function of stellar mass in this model, and the gradient becomes stronger with increasing redshift. The most massive galaxies have resided within group-sized haloes since at least $z = 1.5$; thus any environmental effects would have manifested themselves a long time prior to observation, and we expect to see little signature of cluster growth in their properties. On the other hand, galaxies with lower stellar mass are a better tracer of the recent mass accretion history of the cluster, hence we see a strong evolution in the fraction of environmentally-affected galaxies.

3.5 Observational constraints

It is now useful to review the observational constraints on our model parameters, M_{trunc} and T_{trunc} . The halo mass threshold at which environmental effects become important must be at least as low as $10^{13} h^{-1} M_{\odot}$ because there are observations of systems at this mass with significant environmental effects (Wilman et al. 2005; Weinmann et al. 2006). For this reason, we investigated a model with a low halo mass threshold, $10^{12} h^{-1} M_{\odot}$, in Figure 9. Well defined samples of galaxy clusters show a significant Butcher-Oemler effect, such that the fraction of red galaxies decreases from ~ 0.9 at $z=0.2$ to ~ 0.65 at $z=0.5$ (Ellingson et al. 2001). This evolution is much quicker than predicted by a model with a T_{trunc} of 2 Gyrs or less. Thus a model with M_{trunc} of $\sim 10^{12} h^{-1} M_{\odot}$ and a T_{trunc} of ~ 3 Gyrs is the most favored model. As suggested previously, this leads to the prediction that by $z=1.5$, little or no environmental effects are felt by the galaxy population.

Recall §3.4, in which we investigated the stellar mass dependence of the galaxy population using our most favored model. We found that while the most massive galaxies are environmentally affected at all redshifts, the lower mass galaxies become more affected with time. Gilbank & Balogh (2008) used a compilation of the observational literature to show that the ratio of red bright galaxies to red faint galaxies steadily increases with redshift, the same qualitative behaviour we see in the simple model.

It is difficult to observationally quantify the extent to which massive galaxies are environmentally affected. This is largely because the visual colours of galaxies are not very sensitive to low levels of star formation. Mid-IR observations are more sensitive to low levels of star formation and thus are better at establishing the environmental influence of massive galaxies. Observations at $z \sim 0.4$ suggest that only 10 % of massive galaxies ($> 10^{10} h^{-1} M_{\odot}$) in groups have IR emission indicative of activity, while the global fraction is much higher ($\sim 40\%$, Wilman et al. 2008). Additionally, Wolf et al. (2009) find that massive galaxies are uniformly old and red in the cluster cores, while having a significant population of dusty, star-forming red galaxies in the infall regions. Both of these studies suggests that significant environmental effects are felt even by massive galaxies, as assumed in our model.

We emphasize that this observational comparison is qualitative, yet highly suggestive. In a future paper we investigate the quantitative behavior of these models with a direct comparison to the best available cluster, group and field data to $z \sim 1$.

3.6 Comparison to Previous Work

In an attempt to explain observations of the fraction of cluster members with [OII] emission at $z=0$ and $z=0.6$, Poggianti et al. (2006) have presented a similar, but more complex model. The observations they present (their Figure 4) show that while, at $z=0.6$, higher mass clusters have lower average fractions of [OII] emitting galaxies, this is largely because of an upper envelope which decreases

with increasing cluster velocity dispersion. In contrast, they notice that at $z=0$, the fraction of [OII] emitting galaxies is constant with cluster velocity dispersion above 550 km/s ($\sim 10^{14} h^{-1} M_{\odot}$), but the scatter is large below that value.

In effect, to explain the observations, Poggianti et al. (2006) introduces two M_{trunc} and two T_{trunc} parameters to match the observed behavior. The first set of M_{trunc} and T_{trunc} are meant to represent 'primordially' passive galaxies, and are associated with elliptical galaxies. They claim that galaxies within $3 \times 10^{12} h^{-1} M_{\odot}$ groups at $z = 2.5$ represent these primordially passive galaxies. The second set of parameters are associated with quenched galaxies or S0 galaxies, and are set to have $M_{\text{trunc}}=10^{14} h^{-1} M_{\odot}$ and $T_{\text{trunc}}= 3$ Gyrs. However, observations of galaxy groups with masses less than $10^{14} h^{-1} M_{\odot}$ show a significant population of S0 galaxies and passive spiral galaxies (Wilman et al. 2009, McGee et al., in prep), which are hard to reconcile with their model. On the other hand, the lower value of $M_{\text{trunc}} \sim 10^{13} h^{-1} M_{\odot}$ that we advocate might have trouble explaining the large fraction of galaxies with [OII] emission in the Poggianti et al. (2006) clusters at $z \sim 0.5$. Undoubtedly both models are greatly oversimplified and, moreover, there are important systematic uncertainties in the current data (especially in determining cluster masses and galaxy star formation rates) and statistical limitations resulting from small sample sizes.

Similar constraints have also been derived in the past from observations of radial gradients in clusters. Balogh et al. (2000) used n-body simulations of the infall of substructure into clusters and concluded that, to match the radial gradients of star formation rates, the star formation rates in cluster galaxies must decline on the timescale of a few Gyrs after entering the cluster. Significantly, they also found that the best match to radial gradients was provided if the star formation rate in the galaxy began to decline as soon as it was found in a dark matter structure of group-size or larger. Ellingson et al. (2001) took this a step further and investigated the evolution of such gradients. They determined that 'field-like' galaxies became early type galaxies on a 2-3 Gyr timescale. Ellingson et al. also inferred that if galaxies were transformed on the 3 Gyr timescale, then the galaxy infall rate into clusters between $z \sim 1.5$ and $z \sim 0.5$ must have declined by ~ 20 %. Our results suggest that the infall rate of galaxies into clusters over the same span fell by ~ 15 %. This is a surprisingly good agreement given the large observational uncertainties at each step in this analysis.

Finally, it is instructive to reexamine the results of B09 in the context of our results. We have previously shown that B09 finds a lower fraction of galaxies within groups and clusters than we do (§2.1). This is likely due to a subhalo completeness level which varies as a function of environment. They use the global number density of subhalos above their mass threshold and compare it against SDSS number densities to conclude that their global magnitude limit is $\sim 0.3 L_*$. However, when they compare number densities of their subhalos within clusters with cluster observations, they find that their cluster magnitude limit is $\sim 0.5 L_*$. Using the red galaxy luminosity function derived from a large sample of galaxy clusters by Lu et al. (2009), a magnitude cut of $0.5 L_*$ instead of $0.3 L_*$ reduces the number of cluster galaxies by ~ 40 %. In other words, groups falling into their clusters could have ~ 40 % fewer galaxies than would be expected from a consistent luminosity cut. Indeed, we find that this is on the order of the discrepancy between our results and those of B09. For instance, we have shown that, for $10^{14.2} h^{-1} M_{\odot}$ clusters, ~ 35 % of galaxies have been accreted through $10^{13} h^{-1} M_{\odot}$ halos at $z=0$, while B09

find only 24%. While this disagreement is significant for evaluating the role of preprocessing in cluster assembly, a bigger factor is that the B09 clusters are not very massive. Indeed, these are smaller than the bulk of well studied clusters at intermediate and high redshift. We have extended their analysis to more massive clusters and find, as B09 themselves anticipated, that group pre-processing is potentially much more important for more massive clusters.

3.7 Towards a physically motivated model

We have shown, by following the accretion of galaxies into groups and clusters, and making simple assumptions about the nature of environmental effects on galaxies, that the halo mass at which environmental effects begin to be induced on galaxies is approximately $10^{12} - 10^{13} h^{-1} M_{\odot}$, and the time those effects take to manifest themselves is quite long (> 2 Gyr). Here, we address some of the more important simplifications we have made in constructing this model.

The first simplification is that we have assumed that an environmental effect will have a unique signature on the properties of galaxies. However, in comparing our model to, for instance, the fraction of red galaxies in clusters, we must acknowledge that there is more than one process which can make a galaxy red. In the local Universe, observations suggest that nearly all galaxies with stellar masses above $10^{10} h^{-1} M_{\odot}$ are red regardless of their environment (Baldry et al. 2006). However, as shown in Figure 10, in our simple model the most massive cluster galaxies would still be red, a consequence of the fact that they have resided within massive dark haloes for a long time. This, combined with the fact that the more numerous low mass galaxies dominate the fraction of galaxies in a cluster, indicate that this is not a large complicating factor.

Secondly, we have assumed that all galaxies display environmental effects after a specific time T_{trunc} , regardless of their incoming orbit. However, McCarthy et al. (2008b) has shown in simulations that the environmental effect on an infalling galaxy is dependent on the orbit of that galaxy. McCarthy et al. also showed that the bulk of the environmental effect on an infalling galaxy occurs when the satellite is at its pericentre. The size of this effect can be quantified by the variation in the time it takes a galaxy to fall from the virial radius to the pericentre of its orbit. In Figure 11, we show the distribution of times for a realistic distribution of infalling dark matter substructure from Benson (2005), randomly sampled 10,000 times. The distribution is shown as a mass-independent quantity, along with the best fit gaussian. A cluster of $10^{14} h^{-1} M_{\odot}$ has a $R_{\text{vir}}= 1.26 h^{-1} \text{ Mpc}$ and $V_{\text{circ}}=400 \text{ km/s}$, which translates to a quite narrow distribution, with a dispersion of only ~ 0.2 Gyrs. This will not have significant implications for a timescale which is greater than 2 Gyrs. It is worth noting that the simulations of Benson were not adequate to quantify the effect of any host halo mass dependence of the orbital distribution, but the indications are that this will not have a significant impact for our purposes. Additionally, we have assumed that all galaxies entering a massive halo feel similar environmental effects, however, galaxies with large pericentric distances may not feel strong effects, and thus predictions for the red fraction scatter and its mass dependence will still benefit from proper tracing of orbits in the future.

Thirdly, we have assumed that the mass of a halo is the important quantity driving any environmental effects. In fact, most of the physical processes which could produce environmental effects are likely more sensitive to X-ray gas density or temperature (T_x). For galaxy clusters and massive groups the scatter in the $M-T_x$ relation is actually quite small (± 30 % at $M = 10^{14.5} h^{-1} M_{\odot}$). However,

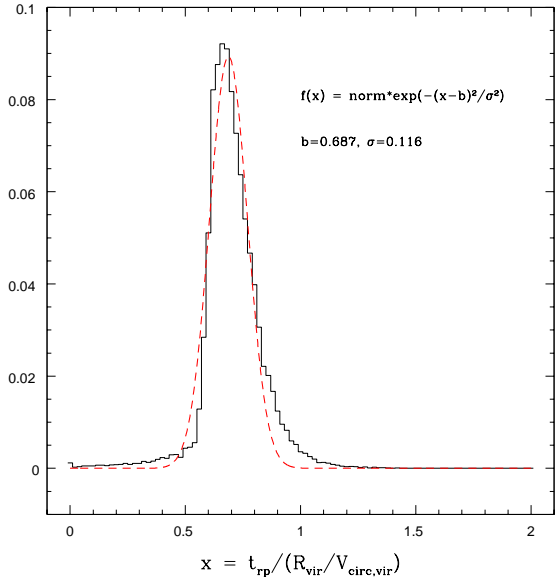


Figure 11. The distribution of times, t_{rp} for an infalling dark matter substructure to reach its pericentre from the virial radius, R_{vir} , of a halo with circular velocity $V_{circ,vir}$. The black line is the distribution of 10^5 randomly sampled orbits from Benson (2005) and the dotted red line is the best fit gaussian.

the Mass – X-ray Luminosity ($M-L$) relation, which is more sensitive to the gas density, does show significant scatter at cluster mass scales (McCarthy et al. 2004; Balogh et al. 2006). But this scatter is driven by properties of the group and cluster cores, while at the radius of a typical galaxy pericentre (0.2-0.3 times the virial radius), the scatter from system to system is quite small (McCarthy et al. 2008a; Sun et al. 2008). So the bulk of ram pressure stripping will occur at radii where the gas density has little scatter from system to system. However, this analysis is limited to fairly massive groups and clusters, as measurement of X-ray properties for typical $10^{12} h^{-1} M_{\odot}$ haloes is quite difficult (Reiprich & Böhringer 2002). One theoretical indication of the size of this effect in low-mass groups comes from the scatter in the virial mass – circular velocity relation, which is approximately $\pm 15\%$ at $M = 10^{12} h^{-1} M_{\odot}$ (Bullock et al. 2001). The circular velocity is more indicative of the depth of the dark matter potential, and thus is likely more closely correlated with the gas density. Despite this, the size of this scatter is likely not a huge source of uncertainty in our model, given that we only make broad statements about the characteristic halo mass scale. Given all of these results, it is encouraging that our model does not appear too simple to give important insights to the behavior of environmental effects.

The next step is to put this ad hoc model on a more physical basis. In particular, in our model we have specified that galaxies within a host halo are equally affected by environmental processes regardless of their position within the halo. But because the cooling rate of gas in a halo is density dependent, semi-analytic models treat galaxies at the center of halos (centrals) different from those not in the center (satellites). While this distinction is still a simplification (Simha et al. 2008), we point out the similarity between a model with a M_{trunc} of $10^{12} h^{-1} M_{\odot}$ and one where the environmental effect begins to occur when a galaxy becomes a satellite, as shown in Figure 8. Our most favored M_{trunc} model is essentially equivalent to choosing a physically motivated central/satellite model.

We have also employed a fixed timescale for environmental effects to occur. Ideally, we would like to link this timescale to a physically motivated quantity, such as the orbital timescale of a galaxy in a cluster or group. This mean timescale is approximately constant for the groups and clusters in our mass range at a given redshift epoch. However, because of the decreasing universe density with time, at high redshift the orbital timescale is actually smaller by a factor of $\sim (1+z)^{3/2}$. A timescale based on this would suggest that at $z=1.5$ the timescale is ~ 4 times shorter than the timescale at $z=0$. Unfortunately, directly implementing a timescale based on the orbital timescale would ignore several other complicating factors such as the evolution of cluster gas density profiles and the evolution of galaxy sizes and densities. Exploring these issues in a full semi-analytic galaxy model is the important next step forward.

4 DISCUSSION AND CONCLUSIONS

We have used the stellar mass and merger trees produced by the semi-analytic galaxy catalogues of F08 to follow the accretion of galaxies into groups and clusters at four different redshift epochs ($z=0, 0.5, 1.0$ and 1.5) for samples of galaxies with stellar mass $M > 10^9 h^{-1} M_{\odot}$. By tracking galaxies through the hierarchy of structure formation we are able to examine the effect that environmental processes may have on the galaxy population of groups and clusters. Further, by adopting a simple model for the environmental effects, we are able to make strong claims about the timescale and mass threshold on which environmental effects occur. Our main results are summarized as follows:

- Clusters at all redshifts examined have had a significant fraction of their galaxies accreted through galaxy groups. For instance, $10^{14.5} h^{-1} M_{\odot}$ mass clusters at $z=0$ have had $\sim 40\%$ of their galaxies ($M_{stellar} > 10^9 h^{-1} M_{\odot}$) accreted through halos with masses greater than $10^{13} h^{-1} M_{\odot}$. At higher redshifts fewer galaxies are accreted through massive halos. Only $\sim 25\%$ of galaxies have been accreted through $10^{13} h^{-1} M_{\odot}$ into $10^{14.5} h^{-1} M_{\odot}$ mass clusters at $z=1.5$.
- We find only a moderate difference in the stellar mass accretion history and the galaxy accretion history at high cluster mass. That is, more massive galaxies are accreted preferentially through groups. While 45% of galaxies in $10^{15} h^{-1} M_{\odot}$ mass clusters at $z=0$ are accreted through halos with masses greater than $10^{13} h^{-1} M_{\odot}$, 50% of the stellar mass is accreted through the same halo mass range. Contrary to the study of Berrier et al. (2009), we do not see a large difference between the galaxy assembly of clusters and the mass assembly of clusters.
- Following from the previous point, we find that the extent to which galaxies are pre-processed in groups before falling into clusters depends on the stellar mass of the infalling galaxy. For a $10^{14.5} h^{-1} M_{\odot}$ mass cluster, 73% of galaxies with stellar masses greater than $10^{10.5} h^{-1} M_{\odot}$ are accreted through $10^{12} h^{-1} M_{\odot}$ systems, while only 50% of 10^9 to $10^{10} h^{-1} M_{\odot}$ are accreted through the same systems. Further, we find that in the accretion through group sized halos increases at late times when compared to the accretion into the cluster during early times.
- We have shown that the fraction of isolated galaxies infalling into $z=0$ groups and clusters is remarkably independent of the final cluster mass. 5-6% of the final cluster galaxies are accreted per Gyr for the last 10 Gyrs. Thus if a galaxy begins to be affected by its environment soon after becoming a satellite galaxy, and the time it takes for that effect to manifest itself is constant with halo mass,

then a similar fraction of galaxies are affected in each cluster above a halo mass of $10^{13} h^{-1} M_{\odot}$.

- Despite the previous result, observing a cluster of the same halo mass at each redshift epoch implies different accretion rates of isolated galaxies, from 5-6 % per Gyr at $z=0$ to 15% per Gyr at $z=1.5$. Thus, in effect, the Butcher Oemler effect may be qualitatively explained by the shorter time available for cluster assembly at higher redshift.

- We find that combining the simple observations of the existence of a significant Butcher Oemler effect at $z=0.5$ and the observations that galaxies within groups display significant environmental effects with galaxy accretion histories justifies striking conclusions. Namely, that the dominant environmental process must begin to occur in halos of $10^{12} - 10^{13} h^{-1} M_{\odot}$ and act over timescales of > 2 Gyrs. This supports a long lifetime, gentle mechanism like strangulation.

- This simple model predicts that by $z=1.5$ galaxy groups and clusters will display little to no environmental effects. This conclusion may have limit the effectiveness of red sequence cluster finding methods at high redshift.

In essence, we have seen that systematic observations of intermediate and high redshift clusters and groups have the power to strongly constrain the mechanisms which induce environmental transformations on galaxies. However, because of the significant cluster to cluster variations in environmental effects, it is important that the method for selecting galaxy clusters and groups for observation must be easily and accurately reproducible in cosmological simulations. Only this will allow the careful testing of models against observations. In a future paper we will compare the best available data on groups and clusters at a variety of redshift epochs to further constrain the dominant environmental processes.

Significant progress on the implications of strangulation and the physical processes involved will need more extensive hydrodynamical simulations. The simulations of ram pressure stripping of the hot haloes of infalling galaxies by McCarthy et al. (2008b) is a significant step forward. However, there are important unknowns. In particular, how effective are low mass group halos in stripping the infalling galaxies? Unfortunately, this is sensitively dependent on how the gas is distributed in both the infalling galaxy and the group halos. Indeed, the effectiveness of strangulation is also dependent on the strength of star formation feedback, and how reheated galaxy gas is distributed and stripped from the galaxy. The behavior of galaxies within small groups which subsequently fall into massive clusters is also unclear. To what extent are galaxies “shielded” by their local group from further gas stripping? Encouragingly, large scale hydrodynamical simulations are beginning to be able to address some of these questions (e.g. Crain et al. 2009).

So, while there is much room for improvement in understanding the details of galaxy – environment interactions, our results have shown that the galaxy accretion histories of groups and clusters combined with a simple model strongly suggest that the dominant environmental effect occurs over long time scales and is effective in low mass halos. In a future paper, we will examine these insights by making a quantitative comparison between semi-analytic models and the best available cluster, group and field data to $z \sim 1$.

ACKNOWLEDGMENTS

We thank the GALFORM team for allowing access to the semi-analytic galaxy catalogues used in this paper and the Virgo Collaboration for carrying out the Millennium simulation. We thank the

referee for comments which improved the paper and we thank Erica Ellingson and Mike Hudson for discussions at an early stage of this work. MLB acknowledges support from an NSERC Discovery Grant. IGM acknowledges support from a Kavli Institute Fellowship.

REFERENCES

- Baldry, I. K., Balogh, M. L., Bower, R. G., Glazebrook, K., Nichol, R. C., Bamford, S. P., & Budavari, T. 2006, MNRAS, 373, 469
- Balogh, M. L., Babul, A., Voit, G. M., McCarthy, I. G., Jones, L. R., Lewis, G. F., & Ebeling, H. 2006, MNRAS, 366, 624
- Balogh, M. L., Baldry, I. K., Nichol, R., Miller, C., Bower, R., & Glazebrook, K. 2004, ApJL, 615, L101
- Balogh, M. L., McGee, S. L., Wilman, D., Bower, R. G., Hau, G., Morris, S. L., Mulchaey, J. S., Oemler, Jr., A., Parker, L., & Gwyn, S. 2009, ArXiv e-prints, 0905.3401
- Balogh, M. L., Morris, S. L., Yee, H. K. C., Carlberg, R. G., & Ellingson, E. 1999, ApJ, 527, 54
- Balogh, M. L., Navarro, J. F., & Morris, S. L. 2000, ApJ, 540, 113
- Benson, A. J. 2005, MNRAS, 358, 551
- Benson, A. J., Bower, R. G., Frenk, C. S., Lacey, C. G., Baugh, C. M., & Cole, S. 2003, ApJ, 599, 38
- Benson, A. J., Kamionkowski, M., & Hassani, S. H. 2005, MNRAS, 357, 847
- Berlind, A. A., Frieman, J., Weinberg, D. H., Blanton, M. R., Warren, M. S., Abazajian, K., Scranton, R., Hogg, D. W., Scocimarro, R., Bahcall, N. A., Brinkmann, J., Gott, J. R. I., Kleinman, S. J., Krzesinski, J., Lee, B. C., Miller, C. J., Nitta, A., Schneider, D. P., Tucker, D. L., & Zehavi, I. 2006, ApJS, 167, 1
- Berrier, J. C., Stewart, K. R., Bullock, J. S., Purcell, C. W., Barton, E. J., & Wechsler, R. H. 2009, ApJ, 690, 1292
- Bond, J. R., Cole, S., Efstathiou, G., & Kaiser, N. 1991, ApJ, 379, 440
- Bower, R. G. 1991, MNRAS, 248, 332
- Bower, R. G., Benson, A. J., Malbon, R., Helly, J. C., Frenk, C. S., Baugh, C. M., Cole, S., & Lacey, C. G. 2006, MNRAS, 370, 645
- Bullock, J. S., Kolatt, T. S., Sigad, Y., Somerville, R. S., Kravtsov, A. V., Klypin, A. A., Primack, J. R., & Dekel, A. 2001, MNRAS, 321, 559
- Butcher, H. & Oemler, Jr., A. 1978, ApJ, 219, 18
- Carlberg, R. G., Yee, H. K. C., Ellingson, E., Abraham, R., Gravel, P., Morris, S., & Pritchet, C. J. 1996, ApJ, 462, 32
- Cole, S., Lacey, C. G., Baugh, C. M., & Frenk, C. S. 2000, MNRAS, 319, 168
- Cooper, M. C., Newman, J. A., Coil, A. L., Croton, D. J., Gerke, B. F., Yan, R., Davis, M., Faber, S. M., Guhathakurta, P., Koo, D. C., Weiner, B. J., & Willmer, C. N. A. 2007, MNRAS, 376, 1445
- Couch, W. J. & Sharples, R. M. 1987, MNRAS, 229, 423
- Crain, R. A., Theuns, T., Dalla Vecchia, C., Eke, V. R., Frenk, C. S., Jenkins, A., Kay, S. T., Peacock, J. A., Pearce, F. R., Schaye, J., Springel, V., Thomas, P. A., White, S. D. M., & Wiersma, R. P. C. 2009, ArXiv e-prints, 0906.4350
- Croton, D. J., Springel, V., White, S. D. M., De Lucia, G., Frenk, C. S., Gao, L., Jenkins, A., Kauffmann, G., Navarro, J. F., & Yoshida, N. 2006, MNRAS, 365, 11
- Davis, M., Efstathiou, G., Frenk, C. S., & White, S. D. M. 1985, ApJ, 292, 371
- Dressler, A. 1980, ApJ, 236, 351

- Dressler, A., Oemler, A. J., Couch, W. J., Smail, I., Ellis, R. S., Barger, A., Butcher, H., Poggianti, B. M., & Sharples, R. M. 1997, *ApJ*, 490, 577
- Eke, V. R., Baugh, C. M., Cole, S., Frenk, C. S., Norberg, P., Peacock, J. A., Baldry, I. K., Bland-Hawthorn, J., Bridges, T., Cannon, R., Colless, M., Collins, C., Couch, W., Dalton, G., de Propris, R., Driver, S. P., Efstathiou, G., Ellis, R. S., Glazebrook, K., Jackson, C., Lahav, O., Lewis, I., Lumsden, S., Maddox, S., Madgwick, D., Peterson, B. A., Sutherland, W., & Taylor, K. 2004, *MNRAS*, 348, 866
- Ellingson, E., Lin, H., Yee, H. K. C., & Carlberg, R. G. 2001, *ApJ*, 547, 609
- Finn, R. A., Balogh, M. L., Zaritsky, D., Miller, C. J., & Nichol, R. C. 2008, *ApJ*, 679, 279
- Font, A. S., Bower, R. G., McCarthy, I. G., Benson, A. J., Frenk, C. S., Helly, J. C., Lacey, C. G., Baugh, C. M., & Cole, S. 2008, *MNRAS*, 389, 1619
- Gerke, B. F., Newman, J. A., Faber, S. M., Cooper, M. C., Croton, D. J., Davis, M., Willmer, C. N. A., Yan, R., Coil, A. L., Guhathakurta, P., Koo, D. C., & Weiner, B. J. 2007, *MNRAS*, 376, 1425
- Gilbank, D. G. & Balogh, M. L. 2008, *MNRAS*, 385, L116
- Gladders, M. D. & Yee, H. K. C. 2000, *AJ*, 120, 2148
- Gómez, P. L., Nichol, R. C., Miller, C. J., Balogh, M. L., Goto, T., Zabludoff, A. I., Romer, A. K., Bernardi, M., Sheth, R., Hopkins, A. M., Castander, F. J., Connolly, A. J., Schneider, D. P., Brinkmann, J., Lamb, D. Q., SubbaRao, M., & York, D. G. 2003, *ApJ*, 584, 210
- Haines, C. P., La Barbera, F., Mercurio, A., Merluzzi, P., & Busarello, G. 2006, *ApJL*, 647, L21
- Hansen, S. M., Sheldon, E. S., Wechsler, R. H., & Koester, B. P. 2007, *ArXiv e-prints*, 0710.3780, 710
- Harker, G., Cole, S., Helly, J., Frenk, C., & Jenkins, A. 2006, *MNRAS*, 367, 1039
- Helly, J. C., Cole, S., Frenk, C. S., Baugh, C. M., Benson, A., & Lacey, C. 2003, *MNRAS*, 338, 903
- Kaiser, N. 1984, *ApJL*, 284, L9
- Kauffmann, G. 1995, *MNRAS*, 274, 161
- Kauffmann, G., Heckman, T. M., Tremonti, C., Brinchmann, J., Charlot, S., White, S. D. M., Ridgway, S. E., Brinkmann, J., Fukugita, M., Hall, P. B., Ivezić, Ž., Richards, G. T., & Schneider, D. P. 2003, *MNRAS*, 346, 1055
- Kauffmann, G., White, S. D. M., & Guiderdoni, B. 1993, *MNRAS*, 264, 201
- Kawata, D. & Mulchaey, J. S. 2008, *ApJL*, 672, L103
- Kenney, J. D. P., van Gorkom, J. H., & Vollmer, B. 2004, *AJ*, 127, 3361
- Kodama, T. & Bower, R. G. 2001, *MNRAS*, 321, 18
- Kubo, J. M., Stebbins, A., Annis, J., Dell'Antonio, I. P., Lin, H., Khabanian, H., & Frieman, J. A. 2007, *ApJ*, 671, 1466
- Lacey, C. & Cole, S. 1993, *MNRAS*, 262, 627
- Lavery, R. J. & Henry, J. P. 1986, *ApJL*, 304, L5
- Lewis, I., Balogh, M., De Propris, R., Couch, W., Bower, R., Offer, A., Bland-Hawthorn, J., Baldry, I. K., Baugh, C., Bridges, T., Cannon, R., Cole, S., Colless, M., Collins, C., Cross, N., Dalton, G., Driver, S. P., Efstathiou, G., Ellis, R. S., Frenk, C. S., Glazebrook, K., Hawkins, E., Jackson, C., Lahav, O., Lumsden, S., Maddox, S., Madgwick, D., Norberg, P., Peacock, J. A., Percival, W., Peterson, B. A., Sutherland, W., & Taylor, K. 2002, *MNRAS*, 334, 673
- Li, Y., Mo, H. J., & Gao, L. 2008, *MNRAS*, 389, 1419
- Lu, T., Gilbank, D. G., Balogh, M. L., & Bognat, A. 2009, *ArXiv e-prints*, 0905.3392
- McCarthy, I. G., Babul, A., Bower, R. G., & Balogh, M. L. 2008a, *MNRAS*, 386, 1309
- McCarthy, I. G., Balogh, M. L., Babul, A., Poole, G. B., & Horner, D. J. 2004, *ApJ*, 613, 811
- McCarthy, I. G., Frenk, C. S., Font, A. S., Lacey, C. G., Bower, R. G., Mitchell, N. L., Balogh, M. L., & Theuns, T. 2008b, *MNRAS*, 383, 593
- McGee, S. L., Balogh, M. L., Henderson, R. D. E., Wilman, D. J., Bower, R. G., Mulchaey, J. S., & Oemler, A. J. 2008, *MNRAS*, 387, 1605
- Natarajan, P., Kneib, J.-P., Smail, I., Treu, T., Ellis, R., Moran, S., Limousin, M., & Czoske, O. 2007, *ArXiv e-prints*, 0711.4587
- Poggianti, B. M., von der Linden, A., De Lucia, G., Desai, V., Simard, L., Halliday, C., Aragón-Salamanca, A., Bower, R., Varela, J., Best, P., Clowe, D. I., Dalcanton, J., Jablonka, P., Milvang-Jensen, B., Pello, R., Rudnick, G., Saglia, R., White, S. D. M., & Zaritsky, D. 2006, *ApJ*, 642, 188
- Press, W. H. & Schechter, P. 1974, *ApJ*, 187, 425
- Reiprich, T. H. & Böhringer, H. 2002, *ApJ*, 567, 716
- Seljak, U. & Zaldarriaga, M. 1996, *ApJ*, 469, 437
- Sheth, R. K. & Tormen, G. 2002, *MNRAS*, 329, 61
- Simha, V., Weinberg, D. H., Dave, R., Gnedin, O. Y., Katz, N., & Keres, D. 2008, *ArXiv e-prints*, 0809.2999
- Somerville, R. S. & Primack, J. R. 1999, *MNRAS*, 310, 1087
- Springel, V. 2005, *MNRAS*, 364, 1105
- Springel, V., White, S. D. M., Jenkins, A., Frenk, C. S., Yoshida, N., Gao, L., Navarro, J., Thacker, R., Croton, D., Helly, J., Peacock, J. A., Cole, S., Thomas, P., Couchman, H., Evrard, A., Colberg, J., & Pearce, F. 2005, *Nature*, 435, 629
- Stewart, K. R., Bullock, J. S., Wechsler, R. H., Maller, A. H., & Zentner, A. R. 2008, *ApJ*, 683, 597
- Sun, M., Voit, G. M., Donahue, M., Jones, C., Forman, W., & Vikhlinin, A. 2008, *ArXiv e-prints*, 0805.2320
- van den Bosch, F. C. 2002, *MNRAS*, 331, 98
- Vollmer, B., Balkowski, C., Cayatte, V., van Driel, W., & Huchtmeier, W. 2004, *A&A*, 419, 35
- Weinmann, S. M., van den Bosch, F. C., Yang, X., & Mo, H. J. 2006, *MNRAS*, 366, 2
- White, S. D. M. & Frenk, C. S. 1991, *ApJ*, 379, 52
- Wilman, D. J., Balogh, M. L., Bower, R. G., Mulchaey, J. S., Oemler, A., Carlberg, R. G., Eke, V. R., Lewis, I., Morris, S. L., & Whitaker, R. J. 2005, *MNRAS*, 358, 88
- Wilman, D. J., Oemler, A., Mulchaey, J. S., McGee, S. L., Balogh, M. L., & Bower, R. G. 2009, *ApJ*, 692, 298
- Wilman, D. J., Pierini, D., Tyler, K., McGee, S. L., Oemler, Jr., A., Morris, S. L., Balogh, M. L., Bower, R. G., & Mulchaey, J. S. 2008, *ApJ*, 680, 1009
- Wolf, C., Aragón-Salamanca, A., Balogh, M., Barden, M., Bell, E. F., Gray, M. E., Peng, C. Y., Bacon, D., Barazza, F. D., Böhm, A., Caldwell, J. A. R., Gallazzi, A., Häußler, B., Heymans, C., Jahnke, K., Jogee, S., van Kampen, E., Lane, K., McIntosh, D. H., Meisenheimer, K., Papovich, C., Sánchez, S. F., Taylor, A., Wisotzki, L., & Zheng, X. 2009, *MNRAS*, 393, 1302
- Zabludoff, A. I. & Mulchaey, J. S. 1998, *ApJ*, 496, 39

APPENDIX: FULL ACCRETION HISTORIES

Here we show the complete accretion histories for each bin of cluster mass and for all four redshift epochs. They are presented for

both the galaxy accretion (Figure 12) and for stellar mass accretion (Figure 13). Figure 12 shows the cumulative distribution of accreted cluster galaxies which reside in a host halo mass of a given size prior to accretion into the final cluster at each of four epochs of observation. Because galaxies are on average more massive in more massive halos, this accretion history does not agree completely with dark matter accretion histories. Therefore, we present the complete stellar mass accretion histories in Figure 13. Again, this shows the cumulative distribution of the accreted stellar mass as a function of the galaxy's host halo mass at the time of accretion.

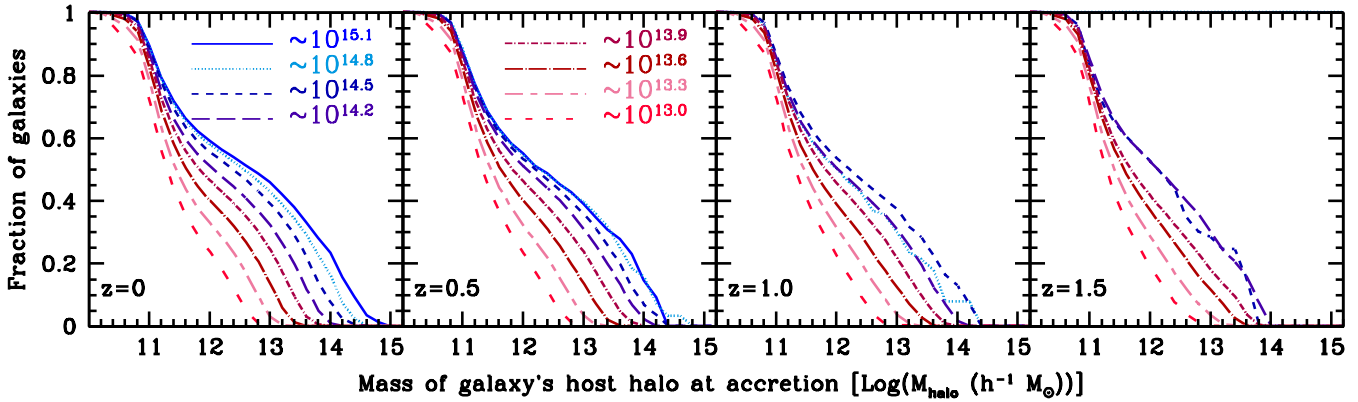


Figure 12. The cumulative distribution of cluster galaxies which reside in a host halo of a given mass at the time of accretion into the final cluster halo. In the left panel is the accretion history of 8 composite clusters of a given final host mass at $z=0$, while in the left middle (right middle) [right] panel is a separate final cluster sample at $z=0.5$ ($z=1$) [$z=1.5$]. All cluster galaxies have final stellar masses of $M > 10^9 M_{\odot}$. The mass range bins were defined in Table 1, and are shown for all bins containing more than one cluster.

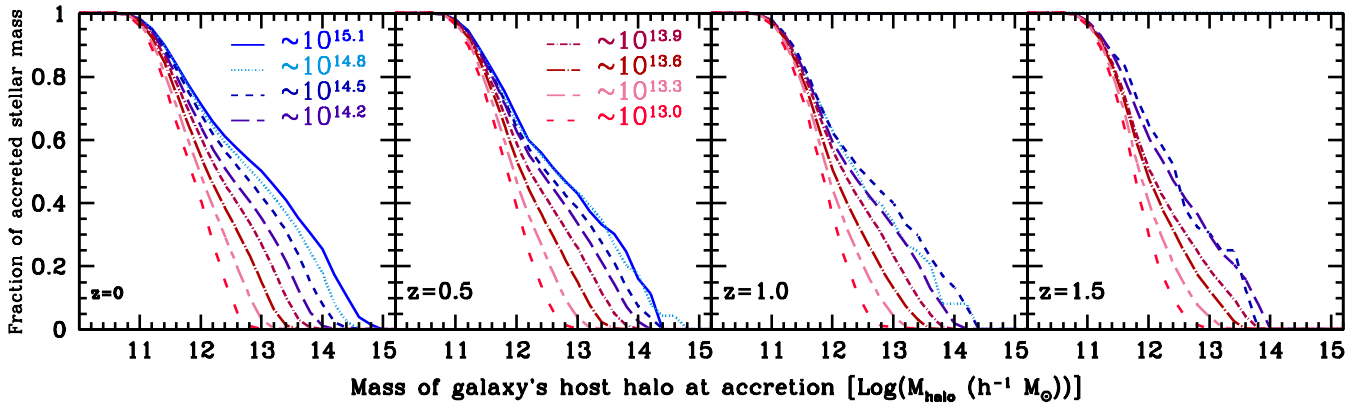


Figure 13. The cumulative distribution of accreted stellar mass which reside in a host halo of a given size at the time of accretion into the final cluster halo. In the left panel, is the accretion history of 8 composite clusters of a given final host mass at $z=0$. The left middle (right middle) [right] panel is for a separate final cluster sample at $z=0.5$ ($z=1$) [$z=1.5$]. All cluster galaxies have final stellar masses of $M > 10^9 M_{\odot}$. The mass range bins were defined in Table 1, and are shown for all bins containing more than one cluster.